Barotropic Continental Shelf Waves on a β-Plane

A. DORR AND R. GRIMSHAW*

Department of Mathematics, University of Melbourne, Parkville, Victoria, 3052 Australia

(Manuscript received 3 September 1985, in final form 30 December 1985)

ABSTRACT

In this paper we consider the effect of the variation of the Coriolis parameter with latitude on barotropic shelf waves, using a β-plane model. Solutions are constructed using the method of inner and outer asymptotic expansions, where the inner expansions hold over the shelf, and the outer expansions hold in the deep ocean. Three cases are identified, depending on the relationship between the shelf wave frequency and the allowed frequencies for deep-ocean Rossby waves. The connection is provided by the matching of the longshore wavenumbers. In the first case, the shelf wave frequency is too large to permit Rossby wave radiation, and the variation of the shelf wave amplitude is governed by conservation of longshore energy flux. In the second case, the shelf wave frequency is sufficiently small to permit Rossby wave radiation at high latitudes, and in the third case there is Rossby wave radiation at all latitudes. In both these cases the longshore shelf wave energy flux decays at a rate determined by the radiated Rossby wave energy flux.

1. Introduction

Current theories for continental shelf waves generally assume that the waveguide is uniform in the longshore direction (see, for instance, Allen, 1980, or Mysak, 1980a). Nevertheless, various authors have considered the effects of longshore variations in bottom topography or coastline curvature (for a recent review, see Mysak, 1980b). However, the effect of variable Coriolis parameter has received less attention. Grimshaw (1977) used a WKB approximation to determine the variation of wave amplitude due to the variation of the Coriolis parameter with latitude but considered only the case when the shelf waves remain trapped in the coastal waveguide. Recently, Beer and Grimshaw (1983) considered continental shelf waves on a β-plane and obtained some analytic solutions for the case when the shelf waves are confined to a channel (i.e., the coastal waveguide is bounded in the offshore direction by a rigid barrier).

Suginohara (1981) found in a numerical experiment that barotropic shelf wave energy leaked away from the coastal region in the form of barotropic Rossby waves. Suginohara and Kitamura (1984) (see also McCreary and Chao, 1985) found a similar phenomenon involving baroclinic Rossby waves in a numerical study of coastal upwelling. Enfield and Allen (1980), in an analysis of sea-level anomalies along the Pacific Coast of America, found that at high latitudes there was significant correlation with local wind stress, but that at low latitudes the anomalies took the form of poleward-propagating waves. It is also relevant to note that Mysak (1983) has recently suggested that baroclinic Rossby waves in the North Pacific may be generated by coastal current oscillations. One factor that may be involved is the variation of the Coriolis parameter and the possible leakage of energy by radiating Rossby waves at high latitudes. Motivated by these papers, we propose to study barotropic continental shelf waves on a β-plane and to quantify the extent to which shelf waves can lose energy by radiation into offshore propagating Rossby waves.

In conventional notation (see Fig. 1), the linearized, nondivergent barotropic shelf-wave equations are

$$u_t - fv + \zeta_x = 0, \tag{1.1a}$$

$$v_t + fu + \zeta_y = 0, \tag{1.1b}$$

$$(hu)_x + (hv)_y = 0. \tag{1.1c}$$

Here we are using nondimensional coordinates based on a length scale L (typical of the shelf width), a time scale F^{-1} where F is a typical value of the Coriolis parameter, and a velocity scale FL; the wave height is scaled by $F^2L^2\ g^{-1}$. Introducing the mass-transport stream function ψ, where

$$hu = \psi_y, \quad hv = -\psi_x, \tag{1.2}$$

and assuming a time dependence proportional to $\exp(-i\omega t)$ (where $\omega > 0$), we find that the vorticity equation is

$$i\omega\left\{\left(\frac{\psi_x}{h}\right)_x + \left(\frac{\psi_y}{h}\right)_y\right\} + \psi_y\left(\frac{f}{h}\right)_x - \psi_x\left(\frac{f}{h}\right)_y = 0. \tag{1.3}$$

We shall assume that the coastline is straight and given by $x = 0$, where ψ must satisfy the boundary condition

$$\psi = 0 \quad \text{at} \quad x = 0. \tag{1.4}$$

* Current address: School of Mathematics, University of N.S.W., Kensington N.S.W. 2033 Australia.

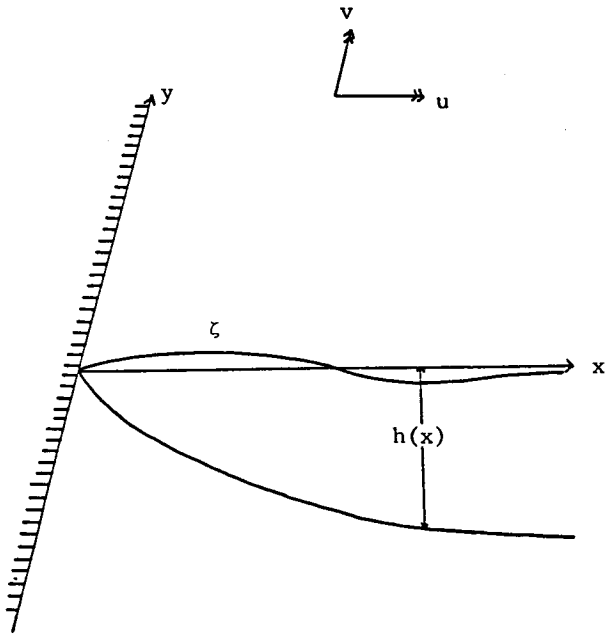

FIG. 1. The coordinate system.

We shall assume that the depth $h = h(x)$ is a monotonically increasing function of x, and that either $h(0) = 0$ with $h_x \neq 0$, or that $h(0) \neq 0$. Also we shall assume that $h \to 1$ exponentially fast as $x \to \infty$, so that $|1 - h|$ is O[exp($-Kx$)] as $x \to \infty$ where K is a positive constant. As $x \to \infty$, ψ must satisfy a radiation condition to ensure that either the waves are trapped or that any radiating waves are outgoing. This radiation condition is developed in section 2.

We shall assume that the variation of the Coriolis parameter f occurs on a length scale much greater than the shelf width. Hence we introduce a small parameter ϵ to measure this slow variation and put

$$f = f_1 + \beta Y + \gamma X, \tag{1.5a}$$

where

$$Y = \epsilon y, \quad X = \epsilon x. \tag{1.5b}$$

Here f_1, β and γ are constants; $\beta > 0$ (<0) corresponds to an east (west) coast. The case $\beta = 0$ corresponds to a coast aligned in the east–west direction; this case will not be considered explicitly in this paper as it has been extensively discussed in the literature on equatorial shelf waves (see, for instance, Beer, 1978, or Mysak, 1978a,b). When $\beta \neq 0$ the longshore wavenumber $m(Y)$ is a function of Y and the aim of the subsequent analysis is to determine $m(Y)$ and the variation of the wave amplitude with Y. In the present nondimensional coordinates the wave phase speed, ωm^{-1}, is O(1) with respect to ϵ, and hence ω and m will have the same order of magnitude. Three cases can be distinguished, depending on whether ω is O(1), O($\epsilon^{1/2}$) or O(ϵ). We designate these cases as follows

I: ω, m are O(1), (1.6a)

II: $\omega = \epsilon^{1/2}\sigma$, $m = \epsilon^{1/2}n$, where σ, n are O(1), (1.6b)

III: $\omega = \epsilon\nu$, $m = \epsilon r$, where ν, r are O(1). (1.6c)

The three cases are analyzed in sections 3, 4 and 5, respectively. In case I the shelf waves are trapped, and the variation of wave amplitude is governed by the conservation of the longshore kinetic energy flux. In case II the shelf waves are trapped at low latitudes but radiate Rossby waves into the deep ocean at high latitudes. In case III the waves radiate at all latitudes, at least in the present β-plane approximation. In each case the solution is constructed as an inner expansion on the shelf where x is O(1) with respect to ϵ. This inner expansion is matched to an outer expansion which holds in the deep ocean, where x is O(ϵ^{-1}) and $h \to 1$. The outer expansion takes the form of modulated Rossby waves, either evanescent or radiating. The theory for these is developed in section 2, where we also describe the matching with the inner expansion.

Before proceeding we note that Willmott and Bird (1983) have considered a similar problem to that formulated here, but for trench waves. (See also Holyer and Mysak, 1985, who consider forcing of trench waves on a β-plane by incident baroclinic Rossby waves.) In effect, the shelf in our formulation is replaced by a depth profile $h(x)$ which at first increases but then decreases as x increases. However, Willmott and Bird (1983) approximated equation (1.3) by replacing f with f_1 in terms such as $f(1/h)x$. This allowed them to keep the longshore wavenumber m constant with the effect that the subsequent analysis is quite different from that presented here. Nevertheless, they also find the existence of regimes in which trench waves radiate energy into the deep ocean.

To conclude this section we consider the equations which describe conservation of energy. These are

$$\langle \zeta\psi_y \rangle_x + \langle -\zeta\psi_x \rangle_y = 0, \tag{1.7a}$$

where

$$\langle ab \rangle = 2\,\mathrm{Re}(ab^*) \tag{1.7b}$$

and is a time average. Equation (1.7a) is readily established from (1.1a, b, c). However, because the geostrophic components of the pressure gradients do no work, Eq. (1.7a) is not a convenient expression to use (see Pedlosky, 1979). Instead we shall use the following expression which can either be derived from (1.7a) using integration by parts and (1.1a, b) or directly from (1.3).

$$F_x + G_y = 0, \tag{1.8a}$$

where

$$F = \left\langle \frac{-\psi\psi_{xt}}{h} - \frac{1}{2}\psi^2\left(\frac{f}{h}\right)_y \right\rangle, \tag{1.8b}$$

$$G = \left\langle \frac{-\psi\psi_{yt}}{h} + \frac{1}{2}\psi^2\left(\frac{f}{h}\right)_x \right\rangle. \tag{1.8c}$$

We shall interpret F and G as the kinetic energy flux in the x- and y-directions, respectively. The radiation condition as $x \to \infty$ is now $F \to 0$ for evanescent waves or that $F > 0$ for radiating waves. In this latter case it can be shown that $F > 0$ is equivalent to the requirement that the x-component of group velocity be positive.

2. Outer expansion: Modulated Rossby waves

The outer expansion holds in the region where $x \sim \epsilon^{-1}$ and $h \sim 1$. In this limit the governing equation (1.3) becomes

$$\psi_{xx} + \psi_{yy} - \frac{\epsilon\beta}{i\omega}\psi_x + \frac{\epsilon\gamma}{i\omega}\psi_y = 0. \tag{2.1}$$

In the outer expansion the appropriate variables are X, Y [see (1.5b)], and the solution has the form of a modulated Rossby wave. Hence we put

$$\psi = A(X, Y)\exp[i\alpha(X, Y)/\epsilon]. \tag{2.2}$$

On substituting (2.2) into (2.1) we find that

$$\alpha_X^2 + \alpha_Y^2 + \frac{\epsilon\beta}{\omega}\alpha_X - \frac{\epsilon\gamma}{\omega}\alpha_Y = \epsilon^2(A_{XX} + A_{YY})/A, \tag{2.3a}$$

$$\left(2\alpha_X + \frac{\epsilon\beta}{\omega}\right)A_X + \left(2\alpha_Y - \frac{\epsilon\gamma}{\omega}\right)A_Y + A(\alpha_{XX} + \alpha_{YY}) = 0. \tag{2.3b}$$

Note that for the three cases I, II and III the terms $\epsilon\gamma/\omega$ and $\epsilon\beta/\omega$ are $O(\epsilon)$, $O(\epsilon^{1/2})$ and $O(1)$, respectively. In all three cases we shall verify a posteriori that the right-hand side of (2.3a) can be neglected, since it is $O(\epsilon^2)$, $O(\epsilon)$ and $O(\epsilon)$, respectively, relative to the left-hand side. The resulting approximation is, in effect, a WKB solution. Matching with the inner solution is achieved by considering the limit $X \to 0$ and will require specification of $\alpha(0, Y)$ and $A(0, Y)$. Hence we impose the boundary conditions

$$\alpha(0, Y) = \theta(Y), \tag{2.4a}$$

$$A(0, Y) = A_0(Y), \tag{2.4b}$$

where $\theta(Y)$ is real-valued.

Equation (2.3a) (with the right-hand side neglected) is the dispersion relation for a Rossby wave of wavenumber (p, q) where

$$p = \alpha_X, \quad q = \alpha_Y, \tag{2.5a}$$

$$p^2 + q^2 + \frac{\epsilon\beta}{\omega}p - \frac{\epsilon\gamma}{\omega}q = 0. \tag{2.5b}$$

Figure 2 shows a plot of the dispersion relation (2.5b) for a fixed frequency ω as a function of (p, q); the arrows point in the direction of increasing ω and define the direction of the group velocity $(\partial\omega/\partial p, \partial\omega/\partial q)$. It will be shown below that the solution of (2.4a) and (2.5a, b) requires q to be real-valued. For a real-valued q the dispersion relation (2.5b) defines two branches. The radiation condition at infinity requires us to choose that branch on which $\mathrm{Im}\,p > 0$ when p is complex-valued corresponding to evanescent waves. When p is real-valued we choose that branch on which $\partial\omega/\partial p > 0$ corresponding to outgoing waves since it can readily be shown that then F (1.8b) is positive. Thus, from (2.5b)

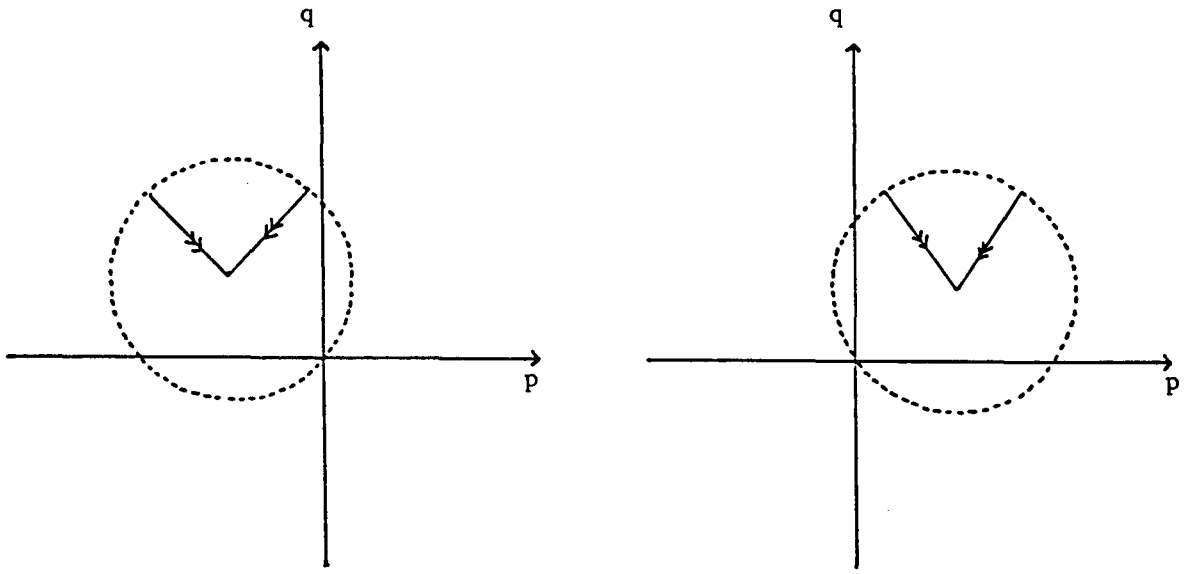

FIG. 2. The Rossby wave dispersion relation, i.e. (2.5b). The arrows point in the direction of increasing ω and define the direction of the group velocity (a) $\beta > 0$ (east coast), (b) $\beta < 0$ (west coast).

$$p + \frac{\epsilon\beta}{2\omega} = f(q) = i\left[\left(q - \frac{\epsilon\gamma}{2\omega}\right)^2 - \frac{\epsilon^2}{4\omega^2}(\beta^2 + \gamma^2)\right]^{1/2}$$

$$\text{if} \quad [\cdots] > 0, \quad (2.6a)$$

or

$$p + \frac{\epsilon\beta}{2\omega} = f(q) = -\left[\frac{\epsilon^2}{4\omega^2}(\beta^2 + \gamma^2) - \left(q - \frac{\epsilon\gamma}{2\omega}\right)^2\right]^{1/2}$$

$$\text{otherwise.} \quad (2.6b)$$

Note that when (2.6b) applies, the radiated Rossby waves have short (long) wavelengths according as $\beta > 0$ (<0), corresponding to the initial condition (2.4a) being applied to an east (west) coast.

The solution of (2.3a) and (2.4a) is achieved by the method of characteristics. First we note that (2.4a) also specifies

$$q(0, Y) = m(Y) = \theta_Y(Y). \quad (2.7)$$

Since (2.3a) contains no explicit dependence on X, Y, both p and q are constant on each characteristic or ray. Thus, on each ray q is real-valued and given by (2.7), and then p is given by (2.6a, b). The rays are given by

$$\frac{dX}{ds} = p + \frac{\epsilon\beta}{2\omega}, \quad \frac{dY}{ds} = q - \frac{\epsilon\gamma}{2\omega}, \quad (2.8a)$$

while

$$\frac{d\alpha}{ds} = -\frac{\epsilon\beta}{2\omega}p + \frac{\epsilon\gamma}{2\omega}q. \quad (2.8b)$$

Here s is a parameter along the ray. The initial conditions for X, Y as $s \to 0$ are $X \to 0$, $Y \to Y_0$. The solution of (2.8a, b) is then

$$Y - Y_0 = \left[m(Y_0) - \frac{\epsilon\gamma}{2\omega}\right]X[f(m(Y_0))]^{-1}, \quad (2.9a)$$

$$\alpha - \theta(Y_0) = -\frac{\epsilon\beta}{2\omega}X + \frac{\epsilon\gamma}{2\omega}(Y - Y_0) + \frac{\epsilon^2}{4\omega^2}\frac{(\beta^2 + \gamma^2)(Y - Y_0)}{m(Y_0) - \frac{\epsilon\gamma}{2\omega}}. \quad (2.9b)$$

Elimination of Y_0 between (2.9a, b) then yields α as function of X, Y. The solution of (2.3b) is now found by integration along the rays. The result is

$$A = J^{-1/2}A_0(Y_0), \quad (2.10a)$$

where

$$J = 1 + Xm_Y(Y_0)\frac{\epsilon^2}{4\omega^2}(\beta^2 + \gamma^2)\{f[m(Y_0)]\}^{-3}. \quad (2.10b)$$

Here J is the Jacobian of the mapping from (s, Y_0) to (X, Y) with the parameter s chosen to ensure that $J = 1$ on the initial line $X = 0$.

Next we consider the matching of the outer expansion (2.2) with the inner expansion, which will be obtained in sections 3 to 5. In the inner expansion the appropriate variables are x and Y. Hence the matching conditions are obtained by putting $X = \epsilon x$ in (2.2) and expanding the result in powers of ϵ with x fixed. We find that

$$\psi(\epsilon x, Y) = \hat{\psi}(x, Y; \epsilon)\exp\left[\frac{i\theta(Y)}{\epsilon}\right], \quad (2.11a)$$

where

$$\hat{\psi}(x, Y; \epsilon) = \left\{A(0, Y) + \epsilon\left[xA_X(0, Y) + \frac{1}{2}ix^2\alpha_{XX}(0, Y)A(0, Y)\right] + O(\epsilon^2)\right\} \times \exp[ip_0(Y)x], \quad (2.11b)$$

where

$$p_0(Y) = p(0, Y). \quad (2.11c)$$

Here $p(0, Y)$ is found from (2.6a, b) with $q = q(0, Y) = m(Y)$. From (2.11b) it follows that

$$\hat{\psi}_x(x, Y; \epsilon) - ip_0(Y)\hat{\psi}(x, Y; \epsilon) = \epsilon\{[A_X(0, Y) + ix\alpha_{XX}(0, Y)A(0, Y)] + O(\epsilon)\}\exp[ip_0(Y)x]. \quad (2.12)$$

We shall find that (2.12) is a more useful form of the matching condition than (2.11b) when considering higher order terms in ϵ.

a. Case I

In this case both ω and m are O(1) with respect to ϵ. It follows that the solution of (2.6a, b) is given by

$$p = i\left|q - \frac{\epsilon\gamma}{2\omega}\right| - \frac{\epsilon\beta}{2\omega} + O(\epsilon^2). \quad (2.13)$$

Thus, to leading order in ϵ, p is pure imaginary, and the waves in the ocean are evanescent. From (2.9a, b) and (2.10a, b) we find that

$$\alpha(X, Y) = \theta(Y + iX) - \frac{\epsilon\beta}{2\omega}X \pm \frac{\epsilon\gamma}{2\omega}iX + O(\epsilon^2), \quad (2.14a)$$

$$A = A_0(Y \pm iX) + O(\epsilon^2), \quad (2.14b)$$

where $\pm$ refers to sign $m(Y)$. The matching conditions (2.11b) and (2.12) become

$$\hat{\psi}(x, Y; \epsilon) = A_0(Y)\exp(-|m|x) + O(\epsilon), \quad (2.15a)$$

$$\hat{\psi}_x(x, Y; \epsilon) + |m|\hat{\psi}(x, Y; \epsilon) = \epsilon\left\{\pm iA_{0Y}(Y) + \left[-ixm_Y(Y) - \frac{i\beta}{2\omega} \pm \frac{\gamma}{2\omega}\right]A_0(Y)\right\} \times \exp(-|m|x) + O(\epsilon^2). \quad (2.15b)$$

Also we note here that α is O(1) with respect to ϵ, and so the right-hand side of (2.3) is $O(\epsilon^2)$ with respect to the left-hand side, thus justifying the formula (2.14a).

b. Case II

In this case ω and m are $O(\epsilon^{1/2})$ with respect to ϵ and hence we replace ω and m with $\epsilon^{1/2}\sigma$ and $\epsilon^{1/2}n$, respectively [see (1.6)]. It follows that p and q are also $O(\epsilon^{1/2})$ and so we put

$$p = \epsilon^{1/2}p_1, \quad q = \epsilon^{1/2}q_1. \tag{2.16}$$

Equations (2.6a, b) become

$$p_1 + \frac{\beta}{2\sigma} = f_1(q_1) = i\left[\left(q_1 - \frac{\gamma}{2\sigma}\right)^2 - \frac{1}{4\sigma^2}(\beta^2 + \gamma^2)\right]^{1/2}, \quad \text{if } [\cdots] > 0, \tag{2.17a}$$

or

$$p_1 + \frac{\beta}{2\sigma} = f_1(q_1) = -\left[\frac{(\beta^2 + \gamma^2)}{4\sigma^2} - \left(q_1 - \frac{\gamma}{2\sigma}\right)^2\right]^{1/2}, \quad \text{otherwise.} \tag{2.17b}$$

If (2.17a) applies, the waves are evanescent, but if (2.17b) applies then there is radiation of outgoing Rossby waves. The demarcation between these two regimes occurs at a critical wavenumber n_c, where $f_1(n_c) = 0$, and is given by

$$n_c = \frac{\gamma}{2\sigma} \pm \left(\frac{\beta^2 + \gamma^2}{4\sigma^2}\right)^{1/2}. \tag{2.18}$$

The two solutions in (2.18) have opposite signs and hence only one can be chosen; waves are evanescent for $n > n_c > 0$ or $n < n_c < 0$ and are radiating otherwise. The equality $n(Y) = n_c$ defines a critical value $Y = Y_c$. Equations (2.9a, b) become

$$Y - Y_0 = \left[n(Y_0) - \frac{\gamma}{2\sigma}\right] X[f_1(n(Y_0))]^{-1}, \tag{2.19a}$$

$$\alpha = \epsilon^{1/2}\left\{\theta_1(Y_0) - \frac{\beta}{2\sigma}X + \frac{\gamma}{2\sigma}(Y - Y_0) + \frac{(\beta^2 + \gamma^2)(Y - Y_0)}{4\sigma^2\left[n(Y_0) - \frac{\gamma}{2\sigma}\right]}\right\}, \tag{2.19b}$$

where $n(Y) = \theta_{1Y}(Y)$, while the amplitude A is again given by (2.10a), but now

$$J = 1 + Xn_Y(Y_0)(\beta^2 + \gamma^2)(4\sigma^2)^{-1}\{f_1[n(Y_0)]\}^{-3}. \tag{2.20}$$

Here we remind the reader that $n(Y)$ is a specified function of Y determined from the inner expansion (see section 4).

We shall show in section 4 that $|n(Y)|$ increases in the equatorward direction (i.e., as $|f_0|$ decreases). Hence when $\beta > 0$ (i.e., on an east coast) and the shelf wave propagates equatorward, there is radiation of Rossby waves until the shelf wave reaches $Y = Y_c$, with a trapped shelf wave thereafter. The pattern of rays forming the radiated Rossby waves is shown in Fig. 3a for the case $f < 0$ (i.e., Southern Hemisphere); for $f > 0$ the pattern is found by taking the mirror image about $Y = Y_c$. The most significant feature of this pattern is the presence of a caustic where $J = 0$, and consequently the amplitude A is infinite [see (2.10a)]. The caustic intersects $X = 0$ at $Y = Y_c$. In the vicinity of the caustic, the outer expansion based on (2.2) fails and must be replaced by an Airy function representation of the wave field (see, for instance, Ludwig, 1966). However, when $\beta < 0$ (i.e., on a west coast) and the shelf wave propagates poleward, there is a trapped wave until the shelf wave reaches $Y = Y_c$, with radiation of Rossby waves

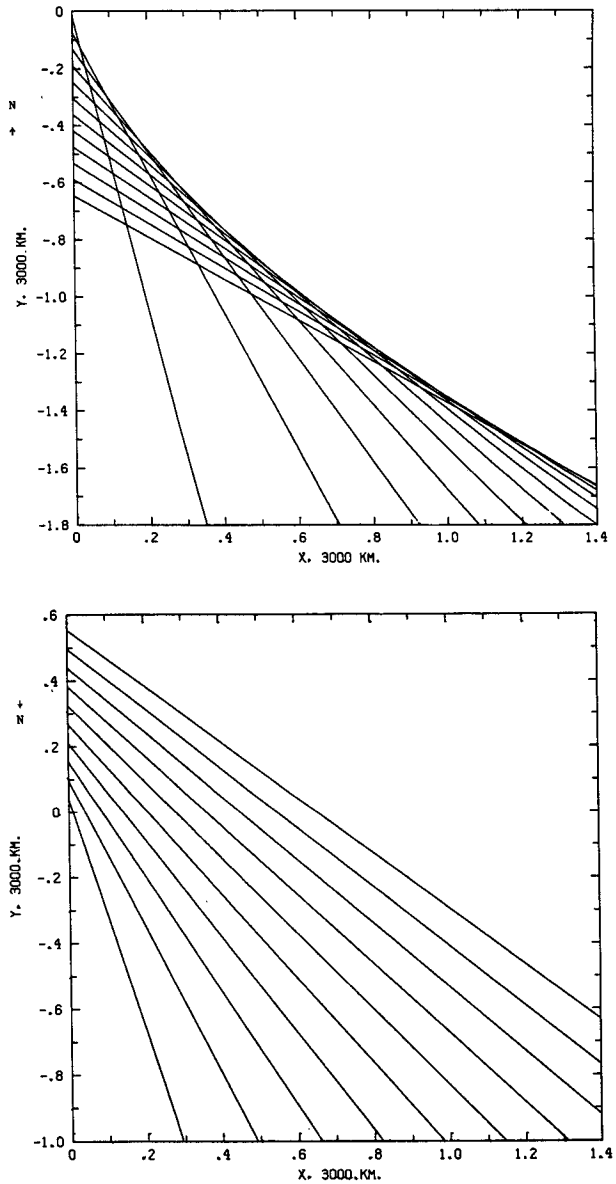

FIG. 3. A typical ray pattern for radiated Rossby waves, shown for the case $f < 0$, and $\gamma = 0$. (a) $\beta > 0$ (east coast); (b) $\beta < 0$ (west coast). In both cases, the shelf wave is propagating in the positive longshore direction and has a period of 15 days; the critical latitude has been placed at $Y = 0$.

thereafter. The pattern of rays is shown in Fig. 3b for the case $f<0$ (for $f>0$ the pattern is the mirror image about $Y=Y_c$). There is now no caustic.

The matching conditions (2.11a) and (2.12) become

$$\hat{\psi}(x, Y; \epsilon) = A_0(Y) + O(\epsilon^{1/2}), \tag{2.21a}$$

$$\hat{\psi}_x(x, Y; \epsilon) - \epsilon^{1/2} i p_{10}(Y)\hat{\psi}(x, Y; \epsilon) = \epsilon A_X(0, Y) + O(\epsilon^{3/2}), \tag{2.21b}$$

where

$$p_{10}(Y) = p_1(0, Y). \tag{2.21c}$$

Here $p_1(0, Y)$ is found from (2.17a, b) with $q_1 = q_1(0, Y) = n(Y)$. We note here that α [see (2.19b)] is $O(\epsilon^{1/2})$ with respect to ϵ, and so the right-hand side of (2.3a) is $O(\epsilon)$ with respect to the left-hand rule. It follows that the error term in (2.1b) is relatively $O(\epsilon)$, or $O(\epsilon^{3/2})$ in total, and thus affects only the error term in (2.21b).

c. *Case III*

In this case ω and m are $O(\epsilon)$ with respect to ϵ, and hence we replace ω and m with $\epsilon\nu$ and ϵr, respectively [see (1.6)]. It follows that q is also $O(\epsilon)$, ϵq_2 say, and hence (2.6a, b) become

$$p = -\frac{\beta}{2\nu} - \left|\frac{\beta}{2\nu}\right| - \frac{\epsilon q_2 \gamma}{|\beta|} + O(\epsilon^2). \tag{2.22}$$

Thus $p \approx -\beta\nu^{-1}$ when $\beta > 0$ (i.e., on an east coast), and p is $O(\epsilon)$ when $\beta < 0$ (i.e., on a west coast). In both cases p is real, and hence only radiating Rossby waves occur. Referring to Fig. 2, we see that with $q \approx 0$, the solutions are $p \approx -\beta\nu^{-1}$ or $p \approx 0$; the former is a short Rossby wave propagating to the east (west) for $\beta > 0$ (<0), and the latter we interpret as a long Rossby wave propagating to the west (east) for $\beta > 0$ (<0). The solution of (2.9a, b) is now

$$\alpha = -\frac{\beta X}{\nu} + \epsilon\theta_2(Y - \gamma\beta^{-1}X) + O(\epsilon^2), \quad \text{if} \quad \beta > 0, \tag{2.23a}$$

$$\alpha = \epsilon\theta_2(Y + \gamma\beta^{-1}X) + O(\epsilon^2), \quad \text{if} \quad \beta < 0, \tag{2.23b}$$

where

$$r(Y) = \theta_{2Y}(Y), \tag{2.23c}$$

while the solution of (2.10a, b) is

$$A = A_0(Y - \gamma\beta^{-1}X), \quad \text{if} \quad \beta > 0, \tag{2.24a}$$

$$A = A_0(Y + \gamma\beta^{-1}X), \quad \text{if} \quad \beta < 0, \tag{2.24b}$$

Note that in the second case, the phase α and the amplitude A are constant along the contours f = constant. The matching conditions (2.11b) and (2.12) now become

$$\hat{\psi}(x, Y; \epsilon) = A(0, Y)\exp\left(-\frac{i\beta x}{\nu}\right) + O(\epsilon), \quad \text{if} \quad \beta > 0, \tag{2.25a}$$

$$\hat{\psi}(x, Y; \epsilon) = A(0, Y) + O(\epsilon), \quad \text{if} \quad \beta < 0. \tag{2.25b}$$

In this case the $O(\epsilon)$ terms in (2.25a, b) will not be needed, and hence we have not displayed them. Finally we note that α [see 2.23a, b)] is either O(1) or $O(\epsilon)$; in the former case the right-hand side of (2.3a) is $O(\epsilon^2)$ relative to the left-hand side, while in the latter case it is $O(\epsilon)$. In both cases (2.23a, b) are consistent with the neglect of the right-hand side of (2.3a).

3. Inner expansion: I—Trapped shelf waves

In this case ω and m are O(1) with respect to ϵ. The inner expansion holds in the region where x is O(1), and the governing equation is (1.3). We seek a solution which has the form of a modulated shelf wave and put

$$\psi = \phi(x, Y; \epsilon)\exp[i\theta(Y)/\epsilon]. \tag{3.1}$$

Here we remind the reader that the longshore wavenumber $m(Y) = \theta_Y(Y)$ [see (2.7)]. Thus ϕ satisfies the equation

$$\left(\frac{\phi_x}{h}\right)_x - \frac{m^2\phi}{h} + \frac{i\epsilon}{h}(2m\phi_Y + m_Y\phi) + \frac{\epsilon^2}{h}\phi_{YY} - \frac{1}{i\omega}\left[\frac{h_x}{h^2}(f_0 + \epsilon\gamma x) - \frac{\epsilon\gamma}{h}\right](im\phi + \epsilon\phi_Y) - \frac{\epsilon\beta}{i\omega h}\phi_x = 0, \tag{3.2a}$$

where

$$f_0(Y) = f_1 + \beta Y. \tag{3.2b}$$

Here $f_0(Y)$ is simply the Coriolis parameter f evaluated at $x = 0$. Also we must satisfy the boundary condition (1.4), or

$$\phi(0, Y; \epsilon) = 0 \tag{3.3}$$

and as $x \to \infty$, ψ must satisfy the matching conditions (2.11a). Thus

$$\phi(x, Y; \epsilon) \sim \hat{\psi}(x, Y; \epsilon) \quad \text{as} \quad x \to \infty \tag{3.4}$$

where $\hat{\psi}$ satisfies (2.11b) and (2.12), which for this present case (i) reduce to (2.15a, b).

We put

$$\phi = \phi_0(x, Y) + \epsilon\phi_1(x, Y) + \cdots, \tag{3.5}$$

and substitute this expansion into (3.2a), (3.3) and (3.4) with the result that

$$\left(\frac{\phi_{0x}}{h}\right)_x - \frac{m^2}{h}\phi_0 - \frac{mf_0}{\omega}\frac{h_x}{h^2}\phi_0 = 0, \tag{3.6a}$$

$$\phi_0 = 0, \quad \text{at} \quad x = 0, \tag{3.6b}$$

$$\phi_0 \sim A_0(Y)\exp(-|m|x) \quad \text{as} \quad x \to \infty. \tag{3.6c}$$

These equations define the shelf wave, and in particular, for a given $h(x)$, determine a set of dispersion relations

$$\omega = -f_0 W(m). \tag{3.7}$$

Some typical dispersion curves, obtained from the exponential depth profile of Buchwald and Adams (1968), are shown in Fig. 4. Since ω is a fixed constant, each dispersion relation (3.7) determines m as a function of Y. Considering only the long wave portion of the dispersion curve (i.e., $|m| < |m_0|$ where m_0 marks the turning point on the dispersion curve) we see that $|m(Y)|$ increases in the equatorial direction (i.e., as $|f_0|$ decreases). For all shelf waves $mf_0 < 0$, and hence on an east coast ($\beta > 0$) the waves propagate equatorward, while on a west coast ($\beta < 0$) the shelf waves propagate poleward. Note that if $m = m_0$ then the group velocity in the Y-direction is zero, and wave reflection will occur. For instance, long shelf waves propagating equatorward on an east coast will reflect into short shelf waves propagating poleward; the opposite process occurs on a west coast. In the vicinity of $m = m_0$ the ansatz (3.1) fails and must be replaced by an expression involving an Airy function; some aspects of this reflection process have been discussed by Beer and Grimshaw (1983) and will not be discussed further here.

At this stage the amplitude of the shelf wave, $A_0(Y)$, is undetermined and is found by considering the equation for ϕ_1. This is

$$\left(\frac{\phi_{1x}}{h}\right)_x - \frac{m^2}{h}\phi_1 - \frac{mf_0}{\omega}\frac{h_x}{h}\phi_1 = g_1, \tag{3.8a}$$

where

$$hg_1 = -i\left(2m\phi_{0Y} + m_Y\phi_0 + \frac{h_x}{h}\frac{f_0}{\omega}\phi_{0Y} + \frac{\beta}{\omega}\phi_{0x}\right) + \frac{\gamma m}{\omega}\left(\frac{xh_x}{h} - 1\right)\phi_0, \tag{3.8b}$$

$$\phi_1 = 0 \quad \text{at} \quad x = 0. \tag{3.8c}$$

The matching condition for ϕ_1 is obtained from (2.15b) and is

$$\phi_{1x} + |m|\phi_1 \sim \left[\pm iA_{0Y} + \left(-ixm_Y - \frac{i\beta}{2\omega} \pm \frac{\gamma}{2\omega}\right)A_0\right] \times \exp(-|m|x) \quad \text{as} \quad x \to \infty. \tag{3.8d}$$

To solve (3.8a) we use the method of variation of parameters. First we let χ_0 be a solution of (3.6a) independent of ϕ_0, defined so that

$$\frac{1}{h}(\phi_{0x}\chi_0 - \chi_{0x}\phi_0) = 1. \tag{3.9}$$

Here the left-hand side is the Wronskian of ϕ_0, χ_0. In particular, it follows from (3.9) that χ_0 cannot satisfy the boundary condition (3.6b) at $x = 0$ and is proportional to $\exp(|m|x)$ as $x \to \infty$. The solution of (3.8a), which satisfies the boundary condition (3.8c), is then

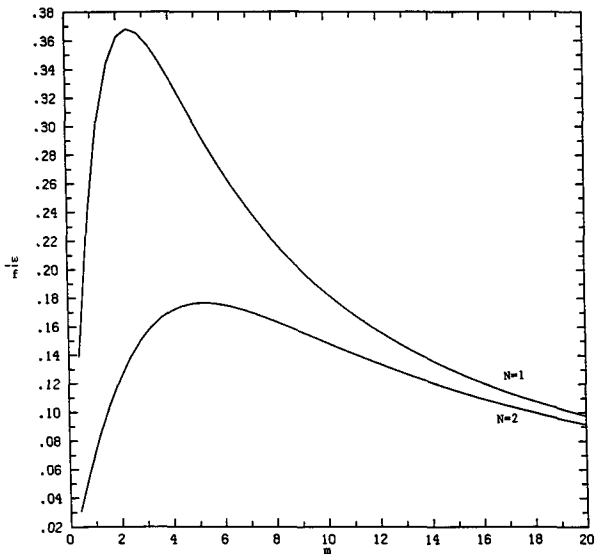

FIG. 4. Typical dispersion curves for the exponential-depth profile [see (3.20) and (3.2a, b, c)]. The curves shown are for $s = 2.0$ and the labels represent the mode number, $N = 1, 2$.

$$\phi_1 = A_1(Y)\phi_0 + \phi_0\int_0^x g_1\chi_0 dx - \chi_0\int_0^x g_1\phi_0 dx. \tag{3.10}$$

Here $A_1(Y)$ is an arbitrary function of Y and represents an $O(\epsilon)$ perturbation of $A_0(Y)$; it does not enter into the subsequent analysis and will be ignored henceforth. In order to satisfy the matching condition (3.8d), the coefficient of χ_0 in (3.10) must be eliminated as $x \to \infty$. Hence we obtain the compatibility condition

$$\int_0^\infty g_1\phi_0 dx = 0. \tag{3.11}$$

From (3.8b) this can be written in the form

$$-\frac{\partial}{\partial Y}\left[\int_0^\infty\left(\frac{2\omega m\phi_0^2}{h} + f_0\frac{h_x}{h^2}\phi_0^2\right)dx\right] = i\gamma m\int_0^\infty\frac{\phi_0^2}{h}\left(\frac{xh_x}{h} - 1\right)dx. \tag{3.12}$$

This is the required equation for the amplitude $A_0(Y)$ and is equivalent to the more general expression obtained by Grimshaw (1977), which included longshore variations in the coastline and depth profile. To conclude, we must now show that the matching condition (3.8d) is satisfied. From (3.10) and (3.11) it follows that

$$\phi_{1x} + |m|\phi_1 \sim (\chi_{0x} + |m|\chi_0) \times \int_x^\infty g_1\phi_0 dx, \quad \text{as} \quad x \to \infty. \tag{3.13}$$

But, from (3.8b) and (3.9) it can be shown that

$$A_0\chi_0 \sim -\frac{1}{2|m|}\exp(|m|x), \quad \text{as} \quad x \to \infty, \tag{3.14a}$$

$$g_1 \sim \left[-i\left(2mA_{0Y} + m_Y A_0 - \frac{\beta|m|}{\omega} A_0 - 2|m|m_Y x A_0\right) - \frac{\gamma m}{\omega} A_0\right] \exp(-|m|x) \quad \text{as} \quad x \to \infty. \quad (3.14b)$$

When (3.14a, b) are substituted into (3.13) we have confirmed that the result is (3.8d).

We next return to (3.12) and note that

$$-\int_0^\infty \left(\frac{2\omega m\phi_0^2}{h} + f_0 \frac{h_x}{h^2}\phi_0^2\right)dx = c_g I, \quad (3.15a)$$

where

$$I = -\frac{f_0 m}{\omega}\int_0^\infty \frac{h_x}{h^2}\phi_0^2 dx, \quad (3.15b)$$

or

$$I = \int_0^\infty \left(\frac{m^2\phi_0^2}{h} + \frac{\phi_{0x}^2}{h}\right)dx. \quad (3.15c)$$

Here $c_g = \partial\omega/\partial m$ is the group velocity. The equality between (3.15b) and (3.15c) is obtained from (3.6a) by multiplication by ϕ_0 and integrating; (3.15a) is then obtained by differentiating with respect to m. From (3.15c) we can show that $|I|$ is the kinetic energy of the shelf wave while it can readily be shown from (1.8c) that $c_g|I|$ is the kinetic energy flux, $\int_0^\infty G dx$. It is apparent from (3.6c) that ϕ_0 is proportional to $A_0(Y)$. Without loss of generality we may put

$$\phi_0(x, Y) = A_0(Y)\tilde{\phi}_0(x, Y) \quad (3.16)$$

where $\tilde{\phi}_0$ is real-valued. Hence $I = A_0^2\tilde{I}$ where $\tilde{I}$ is real-valued and positive and is given by (3.15b or c) with $\tilde{\phi}_0$ in place of ϕ_0. Hence (3.12) becomes

$$\frac{\partial}{\partial Y}(c_g A_0^2 \tilde{I}) = i\gamma m A_0^2 \int_0^\infty \frac{\tilde{\phi}_0^2}{h}\left(\frac{xh_x}{h} - 1\right)dx. \quad (3.17)$$

We now let

$$A_0 = |A_0| \exp\left[i\int_0^Y m_1(Y')dY'\right] \quad (3.18)$$

where m_1 can be regarded as an $O(\epsilon)$ correction to the longshore wavenumber m. Then (3.17) becomes

$$\frac{\partial}{\partial Y}(c_g|A_0|^2\tilde{I}) = 0, \quad (3.19a)$$

$$2m_1(c_g\tilde{I}) = \gamma m \int_0^\infty \frac{\tilde{\phi}_0^2}{h}\left(\frac{xh_x}{h} - 1\right)dx. \quad (3.19b)$$

Here (3.19a) shows that the kinetic energy flux on the Y-direction is constant, while (3.19b) then determines m_1. Note that (3.19a) can also be established from (1.8a, b, c) by integration with respect to x.

For any given depth profile $h(x)$, Eq. (3.19a) determines the variation of shelf wave amplitude $|A_0|$ with f_0. However, it should be pointed out here that $|A_0|$ is the amplitude of the mass transport streamfunction at the shelf break (i.e., as $x \to \infty$ here), and other measures of shelf wave amplitude may be more appropriate. For instance, the wave elevation ζ is given by [see (1.1b)]

$$g\zeta = -\frac{f\psi}{h} - \frac{\omega}{m}\frac{\psi_x}{h}, \quad (3.20)$$

from which it follows that an appropriate measure of wave elevation is $|f_0 A_0|$. For long waves (i.e., $|m| \to 0$), $W(m) \to mc_0$ where c_0 is a positive constant, and hence $|m|$ is proportional to $|f_0|^{-1}$. In the same limit $\tilde{I}$ becomes constant, and $c_g \to -f_0 c_0$; it then follows from (3.19a) that $|A_0|$ is proportional to $|f_0|^{-1/2}$. Thus on an east coast where the waves propagate equatorward the amplitude increases; on a west coast the waves propagate poleward and the amplitude decreases. But note that $|f_0 A_0|$ is proportional to $|f_0|^{1/2}$ and hence the wave elevation decreases equatorward.

To obtain more information it is necessary to specify $h(x)$. We use the exponential-depth profile of Buchwald and Adams (1968). Thus

$$h(x) = \begin{cases} \exp[s(x-1)] & \text{for} \quad 0 \leqslant x \leqslant 1, \\ 1 & \text{for} \quad x \geqslant 1. \end{cases} \quad (3.21)$$

Then we find that

$$\tilde{\phi}_0 = \begin{cases} \dfrac{\sin ax}{\sin a}\exp\left[\dfrac{1}{2}s(x-1)\right] & \text{for} \quad 0 \leqslant x \leqslant 1, \\ \exp[-|m|(x-1)] & \text{for} \quad x \geqslant 1, \end{cases} \quad (3.22a)$$

where

$$a^2 = -\frac{mf_0 s}{\omega} - m^2 - \frac{1}{4}s^2, \quad (3.22b)$$

$$a\cot a = -|m| - \frac{1}{2}s. \quad (3.22c)$$

Equations (3.22b and c) form the dispersion relation (3.7) which is plotted in Fig. 4; this determines m as a function of $|f_0|$. Then from (3.22a) we may calculate $\tilde{I}$ and hence determine $|A_0|$ as a function of $|f_0|$. The results are shown in Fig. 5.

4. Inner expansion: II—Leaky shelf waves

In this case ω and m are $O(\epsilon^{1/2})$ with respect to ϵ and hence we replace them with $\epsilon^{1/2}\sigma$ and $\epsilon^{1/2}n$, respectively [see (1.6b)]. We again seek a solution in the form of a modulated wave (3.1), but we note that $\theta(Y)$ is now $O(\epsilon^{1/2})$. Thus (3.1) and (3.5) are replaced by

$$\psi = \phi(x, Y; \epsilon)\exp[i\theta_1(Y)/\epsilon^{1/2}], \quad (4.1a)$$

$$\phi = \phi_0(x, Y) + \epsilon^{1/2}\phi_1(x, Y) + \cdots. \quad (4.1b)$$

Here n is given by (2.20c). The governing equation is again (3.2a), together with the boundary condition (3.3) and the matching condition (3.4), which now reduces

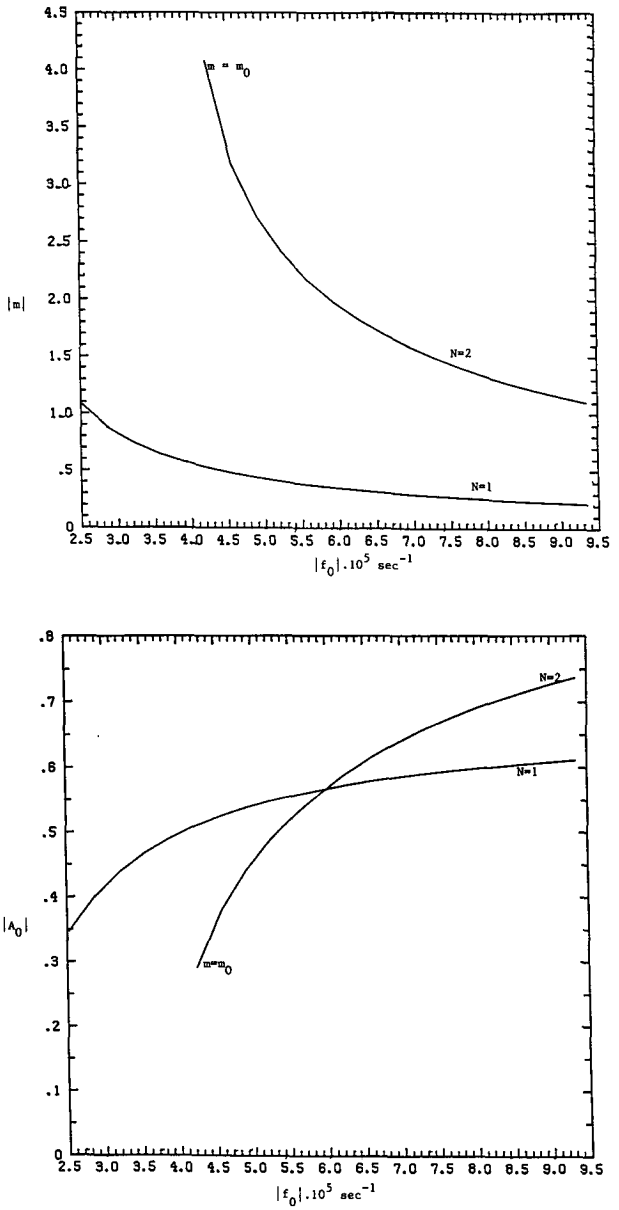

FIG. 5. A plot of the wavenumber $|m|$ and the shelf wave amplitude $|A_0|$ against $|f_0|$ for case I. The curves are shown for the exponential-depth profile (3.20), with $s = 2.0$, for the first two modes and a period of 10 days. Note that mode two has a turning point at $m = m_0$.

to (2.22a, b). On substituting (4.1b) into (3.2a), (3.3) and (3.4) it follows that

$$\left(\frac{\phi_{0x}}{h}\right)_x - \frac{nf_0}{\sigma}\frac{h_x}{h^2}\phi_0 = 0, \tag{4.2a}$$

$$\phi_0 = 0, \quad \text{at} \quad x = 0, \tag{4.2b}$$

$$\phi_0 \sim A_0(Y) \quad \text{as} \quad x \to \infty. \tag{4.2c}$$

Comparing these equations with (3.6a, b, c) we see that they are simply the long-wave limit, $|m| \to 0$, of the shelf wave equations, and in this limit the dispersion relation reduces to

$$\sigma = -f_0 c_0 n, \tag{4.3}$$

where c_0 is a positive constant. Here $|n|$ is proportional to $|f_0|^{-1}$. This result was anticipated in section 2, (ii) and leads to radiating Rossby waves in the ocean when $|n| < |n_c|$ [see (2.18) and the following discussion], and evanescent waves otherwise. The pattern of rays forming the radiated Rossby waves are shown in Fig. 3. Because nf_0/σ is a constant, $\tilde{\phi}_0$ (3.16) is a function of x only.

To determine the amplitude $A_0(Y)$ we must again consider the equation for ϕ_1. This is

$$\left(\frac{\phi_{1x}}{h}\right)_x + \frac{1}{c_0}\frac{h_x}{h^2}\phi_1 = g_1, \tag{4.4a}$$

where

$$hg_1 = -i\left(\frac{f_0}{\sigma}\frac{h_x}{h}\phi_{0Y} + \frac{\beta}{\sigma}\phi_{0x}\right), \tag{4.4b}$$

$$\phi_1 = 0 \quad \text{at} \quad x = 0. \tag{4.4c}$$

The matching condition for ϕ_1 is obtained from (2.21b) and is

$$\phi_{1x} \sim ip_{10}(Y)\phi_0, \quad \text{as} \quad x \to \infty. \tag{4.5}$$

The solution of (4.4a) follows a similar course to that discussed in section 3. Thus let χ_0 be a solution of (4.2a) independent of ϕ_0, defined so that (3.9) again holds. It follows that χ_0 cannot satisfy the boundary condition (4.4c) at $x = 0$ and χ_0 is proportional to x as $x \to \infty$. The solution of (4.4a), which satisfies the boundary condition (4.4c), is then given by (3.10), where now g_1 is given by (4.4b). To satisfy the matching condition (4.5) it follows that

$$-\chi_{0x}\int_0^\infty g_1\phi_0 dx \sim ip_{10}A_0, \quad \text{as} \quad x \to \infty. \tag{4.6}$$

But, from (3.9) it can be shown that

$$-A_0\chi_{0x} \sim 1 \quad \text{as} \quad x \to \infty. \tag{4.7}$$

Thus the compatibility condition (4.6) becomes

$$\int_0^\infty g_1\phi_0 dx = ip_{10}A_0^2. \tag{4.8}$$

Using (2.17a, b) and (4.4b) this becomes

$$-\frac{\partial}{\partial Y}\left(\int_0^\infty f_0\frac{h_x}{h^2}\phi_0^2 dx\right) = 2\sigma f_1(n)A_0^2 \tag{4.9}$$

and is the required equation for the amplitude A_0. Here $f_1(n)$ is defined by (2.17a, b).

In order to interpret (4.9) we first note that

$$I = \int_0^\infty \frac{\phi_{0x}^2}{h}dx = \frac{1}{c_0}\int_0^\infty \frac{h_x}{h^2}\phi_0^2 dx. \tag{4.10}$$

This is readily established from (4.2a, b, c) and is the

long-wave limit of the relations (3.15b, c). Thus $|I|$ measures the kinetic energy of the shelf wave. We let

$$\phi_0(x, Y) = A_0(Y)\tilde{\phi}_0(x), \tag{4.11a}$$

$$A_0 = |A_0| \exp\left(i \int_0^Y n_1(Y')dY'\right), \tag{4.11b}$$

which are the counterparts of (3.15) and (3.17) for the long-wave limit. Here n_1 is an $O(\epsilon^{1/2})$ correction to the longshore wavenumber n. Then (4.9) becomes

$$\frac{\partial}{\partial Y}[f_0|A_0|^2]\frac{c_0\tilde{I}}{2\sigma} = -[\mathrm{Re}f_1(n)]|A_0|^2, \tag{4.12a}$$

$$n_1 f_0|A_0|^2 \frac{c_0\tilde{I}}{\sigma} = -[\mathrm{Im}f_1(n)]|A_0|^2. \tag{4.12b}$$

Here the real and imaginary parts of $f_1(n)$ are obtained from (2.17a, b) and $\tilde{I}$ is a real-valued, positive constant and is given by (4.10) with $\tilde{\phi}_0$ in place of ϕ_0. Equation (4.12a) shows that the kinetic energy flux is constant when the waves are evanescent in the ocean but decays when there is radiation of Rossby waves into the ocean. It can also be established from (1.8a, b, c) by integration with respect to x. On an east coast the shelf waves propagate equatorward and the kinetic energy flux decays until the waves reach $Y = Y_c$ (where $n = n_c$), after which the kinetic energy flux is constant. On a west coast the shelf waves propagate poleward, and the kinetic energy flux is constant until $Y = Y_c$ with decay thereafter. Equation (4.12a) can be integrated to give

$$f_0|A_0|^2 = (\text{constant}) \times \exp\left\{\frac{2\sigma}{\beta c_0\tilde{I}}\int_n^{n_c}\left[\frac{\beta^2+\gamma^2}{4\sigma^2} - \left(n - \frac{\gamma}{2\sigma}\right)^2\right]^{1/2}\frac{dn}{n}\right\},$$

$$\text{if} \quad [\cdots] > 0, \tag{4.13a}$$

$$f_0|A_0|^2 = \text{constant, otherwise.} \tag{4.13b}$$

Here we recall that n is a function of Y by virtue of (3.2b) and (4.3). In Fig. 6 we show a graph of (4.13a) for the special case when $\gamma = 0$ and $h(x)$ is given by the exponential-depth profile of Buchwald and Adams (1968) [see (3.21)]. Here $\tilde{\phi}_0$ is given by the long-wave limit of (3.21a), and we find that

$$\tilde{\phi}_0 = \begin{cases} \dfrac{\sin ax}{\sin a}\exp\left[\dfrac{1}{2}s(x-1)\right], & \text{for} \quad 0 \leqslant x \leqslant 1, \\ 1, & \text{for} \quad x \geqslant 1, \end{cases} \tag{4.14a}$$

where

$$c_0 = s\left(a^2 + \frac{1}{4}s^2\right)^{-1}, \tag{4.14b}$$

$$a\cot a = -\frac{1}{2}s. \tag{4.14c}$$

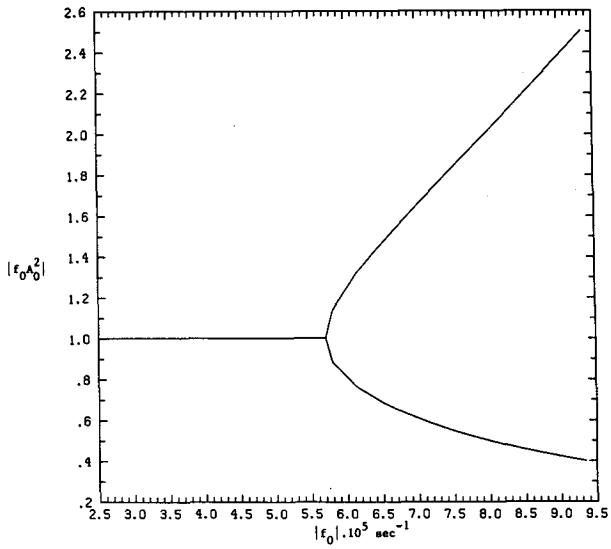

FIG. 6. A plot of the kinetic energy flux $|f_0A_0^2|$ (4.13a, b) against $|f_0|$ for case II. The curves are shown for the exponential-depth profile (3.20), with $s = 2.0$, $\gamma = 0$, for the first mode and a period of 15 days.

The critical value Y_c is found by substituting (4.3) into (2.18). With $\gamma = 0$ this gives

$$|f_{0c}| = 2\sigma^2|\beta c_0|^{-1}, \quad f_{0c} = f_1 + \beta Y_c. \tag{4.15}$$

The critical latitude thus decreases with the square of the shelf wave frequency and inversely with the shelf width, L; the latter result follows here since β is a nondimensional quantity which scales with the shelf width. For instance with $L = 100$ km, $s = 3$ and a dimensional value of $\beta = 2 \times 10^{-11}$ m^{-1} s^{-1}, we find that the critical inertial period is 0.59 days (or a critical latitude of 58°) for a mode-one shelf wave of period 10 days, and a critical inertial period of 1.33 days (or a critical latitude of 22.5°) for a mode-one shelf wave of period 15 days. For the same parameters a mode-two shelf wave has critical inertial periods of 0.15 days and 0.34 days, respectively; since these are less than the minimum allowable inertial period of 0.5 days, there is no radiation. With these parameters, the minimum period for radiation from a mode-two shelf wave is 18.2 days, while for a mode one shelf wave the minimum period is 9.2 days. Returning to Fig. 6, it can be shown that the exponent in (4.13a) is a function of f_0/f_{0c}, $c_0\tilde{I}$ and the ratio γ/β and, in particular, is independent of the wave period σ. The value $c_0\tilde{I}$ is a function of the slope s alone, and with $s = 3$ it can be seen from Fig. 6 that loss of energy by radiation can be significant. Also, $c_0\tilde{I}$ decreases as s decreases and consequently the loss of energy by radiation increases.

5. Inner expansion: III—Modified topographic Rossby waves

In this case ω and m are $O(\epsilon)$ with respect to ϵ and hence we replace them with $\epsilon\nu$ and ϵr, respectively [see

(1.6c)]. We again seek a solution in the form of modulated wave (3.1), but we note that now $\theta(Y)$ is $O(\epsilon)$. Hence (3.1) is replaced by

$$\psi = \phi(x, Y; \epsilon) \exp[i\theta_2(Y)], \tag{5.1}$$

where r is given by (2.23c). The governing equation is again (3.2a), together with the boundary condition (3.3) and the matching condition (3.4) which now reduces to (2.25a, b). We now let ϕ have the expansion (3.5) and substitute the result into (3.2a), (3.3) and (3.4). Without any loss of generality we also let ϕ_0 be given by (3.16) and assume that both $r(Y)$ and $A_0(Y)$ are real-valued. Then we find that

$$\left(\frac{\tilde{\phi}_{0x}}{h}\right)_x - \frac{f_0}{\nu}\left(r - i\frac{A_{0Y}}{A_0}\right)\frac{h_x}{h^2}\tilde{\phi}_0 + \frac{i\beta}{\nu h}\tilde{\phi}_{0x} = 0, \tag{5.2a}$$

$$\tilde{\phi}_0 = 0, \quad \text{at} \quad x = 0, \tag{5.2b}$$

$$\tilde{\phi}_0 \sim \begin{cases} \exp\left(-\dfrac{i\beta x}{\nu}\right), & \text{if } \beta > 0 \\ 1, & \text{if } \beta < 0 \end{cases} \quad \text{as } x \to \infty. \tag{5.2c}$$

Since $\tilde{\phi}_0$ is a function of x only, the dispersion relation is

$$\nu = -f_0 c_0\left(r - i\frac{A_{0Y}}{A_0}\right), \tag{5.3}$$

where c_0 is a *complex-valued* constant. Thus (5.2a) becomes

$$\left(\frac{\tilde{\phi}_{0x}}{h}\right)_x + \frac{1}{c_0}\frac{h_x}{h^2}\tilde{\phi}_0 + \frac{i\beta}{\nu h}\tilde{\phi}_{0x} = 0. \tag{5.4}$$

Comparing (5.4) with (4.2a) we see that (5.4) can be regarded as the long-wave equation (4.2a) modified by the inclusion of the term involving β, which has the effect of causing the "speed" c_0 to be a complex-valued constant. Once c_0 has been determined, r and A_0 are found from (5.4). We put

$$A_0 = (\text{constant}) \exp\left[-\int_0^Y \rho(Y')dY'\right], \tag{5.5a}$$

$$R = r + i\rho. \tag{5.5b}$$

Then (5.3) reduces to

$$\nu = -f_0 c_0 R, \tag{5.6}$$

which shows that R is proportional to f_0^{-1}. Also we note from (5.1) and (5.5a, b) that

$$\psi = \tilde{\phi}_0(x) \exp\left[i\int_0^Y R(Y')dY'\right]. \tag{5.7}$$

To determine c_0 we must specify $h(x)$ and then solve (5.4) with the boundary conditions (5.2b, c). First, however, we derive some general results. If we multiply (5.4) by $\tilde{\phi}_0^*$, and then subtract the complex conjugate of the result, we can show that

$$\frac{\partial}{\partial x}\left[\frac{(\tilde{\phi}_0^*\tilde{\phi}_{0x} - \tilde{\phi}_0\tilde{\phi}_{0x}^*)}{h} + \frac{i\beta}{\nu h}|\tilde{\phi}_0|^2\right] + \left[\frac{1}{c_0} - \frac{1}{c_0^*} + \frac{i\beta}{\nu}\right]\frac{h_x}{h^2}|\tilde{\phi}_0|^2 = 0. \tag{5.8}$$

Integration, and use of the boundary conditions (5.2b, c) then gives

$$\left[\beta + 2\nu\,\mathrm{Im}\left(\frac{1}{c_0}\right)\right]\int_0^\infty \frac{h_x}{h^2}|\tilde{\phi}_0|^2 dx = |\beta|. \tag{5.9}$$

This result can also be obtained directly from (1.8a, b, c) by integration with respect to x and hence is an expression of the conservation of kinetic energy. Further, it can be shown that the kinetic energy flux in the Y-direction is given by

$$\int_0^\infty G dx = -f_0 A_0^2 \int_0^\infty \frac{h_x}{h^2}|\tilde{\phi}_0|^2 dx. \tag{5.10}$$

Thus these waves, like shelf waves, propagate equatorward (poleward) on an east (west) coast. From (5.9) it follows that

$$\beta + 2\nu\,\mathrm{Im}\left(\frac{1}{c_0}\right) > 0. \tag{5.11}$$

Using (5.5a, b) and (5.6) it can now be shown that (5.11) is precisely the condition needed to ensure that the kinetic energy flux decays in the direction of propagation. Indeed it can be shown from (5.5a, b), (5.6) and (5.10) that the kinetic energy flux is proportional to $|f_0|^b$, where

$$b = 1 + \frac{2\nu}{\beta}\,\mathrm{Im}\left(\frac{1}{c_0}\right).$$

From (5.10) we note that

$$b = \mathrm{sgn}\beta\left(\int_0^\infty \frac{h_x}{h^2}|\tilde{\phi}_0|^2 dx\right)^{-1};$$

using this form for the kinetic energy flux it is readily shown that in the limit $\beta/2\nu \to 0$ the results of this section agree with those of case II (§4) in the limit $\sigma/\beta \to 0$ [see, for instance, (4.12a)].

Next we put

$$\tilde{\phi}_0 = \chi_0 \exp\left(-\frac{i\beta x}{\nu}\right) \tag{5.12}$$

and substitute this expression into (5.2b, c) and (5.4). We find that

$$\left(\frac{\chi_{0x}}{h}\right)_x + \left(\frac{1}{c_0} + \frac{i\beta}{\nu}\right)\frac{h_x}{h^2}\chi_0 - \frac{i\beta}{\nu h}\chi_{0x} = 0, \tag{5.13a}$$

$$\chi_0 = 0, \quad \text{at} \quad x = 0, \tag{5.13b}$$

$$\chi_0 \sim \begin{cases} 1, & \text{if } \beta > 0 \\ \exp\left(\dfrac{i\beta x}{\nu}\right), & \text{if } \beta < 0 \end{cases} \quad \text{as } x \to \infty. \tag{5.13c}$$

It follows that if $[\tilde{\phi}_0(x;\beta); 1/c_0(\beta)]$ is a solution pair then so is

$$\left[\chi_0(x;-\beta); \frac{1}{c_0(-\beta)} - \frac{i\beta}{\nu}\right].$$

Hence we deduce that

$$\frac{1}{c_0(\beta)} = \frac{1}{c_0(-\beta)} - \frac{i\beta}{\nu}. \tag{5.14}$$

Thus, it is sufficient to calculate c_0 for $\beta > 0$.

The first specific case we consider is that for the step-depth profile, where

$$h(x) = \begin{cases} h_0 & \text{for } x < 1 \\ 1 & \text{for } x > 1. \end{cases} \tag{5.15}$$

At the discontinuity $x = 1$, $\tilde{\phi}_0$ must satisfy the discontinuity relations

$$[\tilde{\phi}_0]_-^+ = 0, \quad \left[\frac{1}{h}\left(\tilde{\phi}_{0x} - \frac{1}{c_0}\tilde{\phi}_0\right)\right]_-^+ = 0. \tag{5.16}$$

We find that

$$\tilde{\phi}_0 = \frac{\sin\left(\dfrac{\beta x}{2\nu}\right)}{\sin\left(\dfrac{\beta}{2\nu}\right)} \exp\left(-\frac{i\beta x}{\nu} - \frac{i|\beta|}{2\nu}\right), \quad \text{for } x < 1, \tag{5.17}$$

and is given by (5.2c) for $x > 1$, while

$$\frac{1}{c_0}(1 - h_0) = \frac{\beta}{2\nu}\cot\frac{\beta}{2\nu} - \frac{i\beta}{2\nu}(1 - h_0) + ih_0\frac{|\beta|}{2\nu}. \tag{5.18}$$

Note that $\mathrm{Re}(1/c_0)$ is zero for $\beta/\nu = \pm\pi, \pm 3\pi, \cdots$; this corresponds to a zero value for the wavenumber r, and the solution represents a stationary oscillation. Also $\mathrm{Re}(1/c_0)$ is infinite for $\beta/\nu = \pm 2\pi, \pm 4\pi, \cdots$; this corresponds to an infinite value for the wavenumber r, and the solution represents a resonant oscillation on the shelf [see (5.17)].

The second case we consider is the exponential-depth profile (3.20), for which we find that

$$\tilde{\phi}_0 = \frac{\sin ax}{\sin a} \exp\left\{\frac{1}{2}\delta(x-1)\right\}, \quad \text{for } x < 1, \tag{5.19a}$$

where

$$\delta = s - \frac{i\beta}{\nu}, \tag{5.19b}$$

$$a^2 = \frac{s}{c_0} + \frac{\beta^2}{4\nu^2} - \frac{s^2}{4} + \frac{is\beta}{2\nu}, \tag{5.19c}$$

and is given by (5.2c) for $x > 1$. Application of (5.16) then gives

$$a\cot a = -\frac{1}{2}s - \frac{i|\beta|}{2\nu}. \tag{5.20}$$

The "speed" c_0 is found by solving (5.20) for a, and then evaluating c_0 from (5.19c). The results are displayed in Fig. 7, which shows $1/c_0$ as a function of $\beta/2\nu$ for various values of s and for the first two modes. As in the first case there are values of β/ν where $\mathrm{Re}(1/c_0)$ is zero, corresponding to a zero value of r and a stationary oscillation. However, infinite values of $\mathrm{Re}(1/c_0)$ cannot now occur. It is also interesting to note

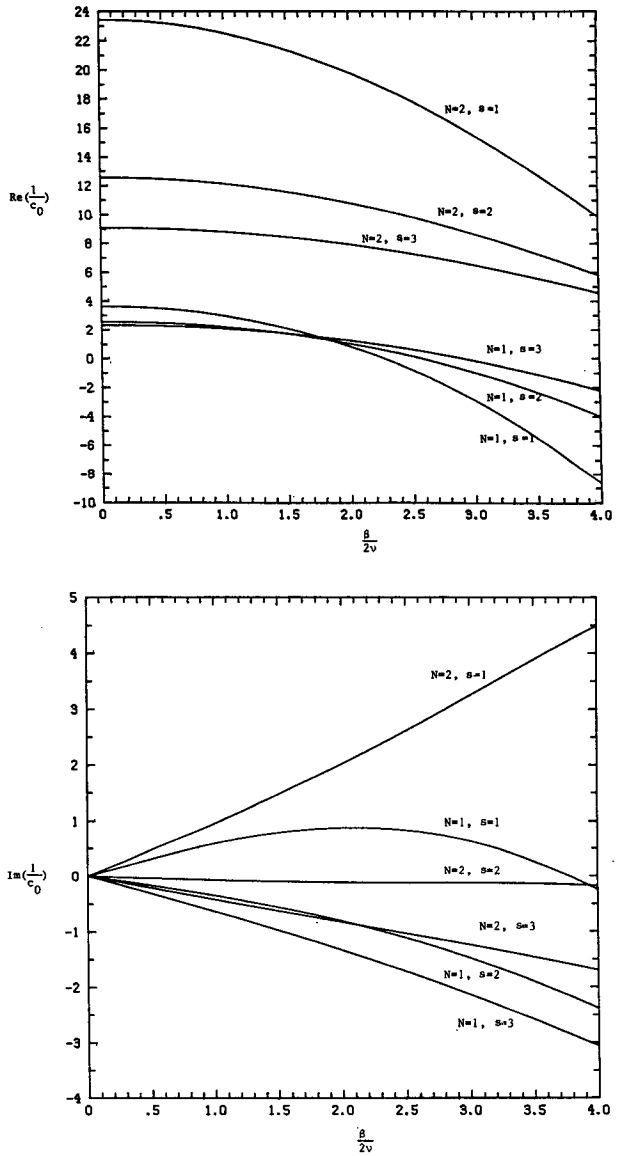

FIG. 7. A plot of $1/c_0$ against $\beta/2\nu$ for case III, $N = 1, 2$. The curves are shown for the exponential-depth profile (3.20), for $s = 1.0$, 2.0 and 3.0. (a) $\mathrm{Re}(1/c_0)$; (b) $\mathrm{Im}(1/c_0)$.

that for sufficiently large values of β/ν, $\mathrm{Re}(1/c_0)$ is negative, implying phase propagation in the opposite sense to energy propagation [which is equatorward (poleward) on an east (west) coast; see (5.10)]. In Fig. 8 we show a plot of the kinetic energy flux (5.10) as a function of Y.

To conclude this section we note the consequences of replacing the radiation condition (5.2c) with

$$\tilde{\phi}_0 \sim \begin{cases} 1, & \text{if } \beta > 0 \\ \exp -\left(\dfrac{i\beta x}{\nu}\right), & \text{if } \beta < 0 \end{cases} \quad \text{as } x \to \infty. \quad (5.21)$$

This corresponds to incoming waves from infinity, and the solution of (5.2a, b) with (5.21) describes an oceanic Rossby wave which is incident on the continental shelf and is effectively absorbed there since there is no reflection. The kinetic energy flux generated on the shelf now grows in the direction of propagation. If $[\tilde{\phi}_0(x;\beta); 1/c_0(\beta)]$ is a solution of (5.2a, b) and (5.2c) then it can be shown that $[\tilde{\phi}_0^*(x,-\beta); 1/c_0^*(-\beta)]$ is a solution of (5.2a, b) and (5.21). Hence the solution for these amplifying waves can be found from the solution for the leaky waves by replacing c_0 with c_0^* and β with $-\beta$.

More general solutions to (5.2a, b) can be constructed for which the radiation condition (5.2c) is replaced by a condition which describes a combination of incident and reflected oceanic Rossby waves. For this more general case the "speed" c_0 can be specified a priori and, in particular, can be chosen to be real-valued so that the longshore wavenumber R (5.6) is also real-valued and the solution (5.7) does not decay or grow in the longshore direction. The result of such a calculation would determine the reflection coefficient as a function of R and the parameters defining the depth profile. This is the procedure followed by Holyer and Mysak (1985) in discussing baroclinic Rossby waves incident on a trench. We shall not pursue this line of inquiry any further, but we note that the case when the incident (or reflected) wave amplitude is zero produces the solutions described in this section.

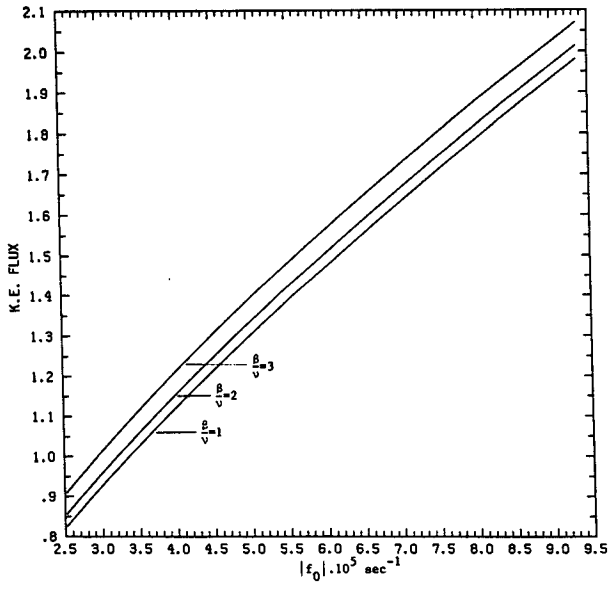

FIG. 8. A plot of the kinetic energy flux (5.10) against $|f_0|$ for case III. The curves are shown for the exponential-depth profile (3.20), with $s = 2.0$, for $\beta/\nu = 1.0$, 2.0 and 3.0.

6. Conclusions

In this paper we have considered the effect of the variation of the Coriolis parameter with latitude on barotropic shelf waves within the context of a β-plane model. Three cases have been identified which depend on the relationship between the shelf wave frequency and the range of frequencies permitted by the deep-ocean Rossby wave dispersion relation. The connection is provided by the requirement that longshore shelf wave wavenumber should match the corresponding wavenumber component of the deep-ocean Rossby waves. In the first case (I) the shelf wave frequency is too large to permit the generation of deep-ocean Rossby waves, the shelf waves are trapped at the coast, and the variation of shelf wave amplitude is governed by the conservation of energy flux in the longshore direction. The main result is (3.18a), which is graphed in Fig. 5 for the exponential-depth profile. For long waves, conservation of energy flux implies that the mass transport streamfunction varies as $|f_0|^{-1/2}$ and the wave elevation varies as $|f_0|^{1/2}$ where f_0 is the Coriolis parameter at the coast. In the second case (II) the shelf wave frequency is small enough to permit some generation of deep-ocean Rossby waves. The shelf waves are trapped at low latitudes but radiate Rossby waves into the deep ocean at high latitudes. The critical latitude which separates these two regimes is given by (2.18) where the critical wavenumber is found from (4.3). In dimensional variables the critical latitude is thus given by

$$\frac{2\omega^2}{|f_0 c_0|} = \gamma \,\mathrm{sgn} f_0 + [\beta^2 + \gamma^2]^{1/2} \quad (6.1)$$

where ω is the wave frequency, c_0 is the long-wave phase speed, and β and γ are derivatives of the Coriolis parameter in the longshore and offshore directions, respectively. The variation of shelf wave amplitude in high latitudes is governed by the requirement that the longshore shelf wave energy flux decay at the rate determined by the radiated Rossby wave energy flux; at low latitudes the longshore energy flux is conserved. The main result is (4.13a, b), which for the exponential-depth profile is graphed in Fig. 6. In the third case (III) the shelf wave frequency is sufficiently low to generate deep-ocean Rossby waves at all latitudes. The main result is described by (5.6) and (5.7) where the complex constant c_0 is determined by solving (5.4). For the ex-

ponential-depth profile, c_0 is graphed in Fig. 7. Although all our calculations have been for a β-plane model we would expect to obtain qualitatively similar results for a more sophisticated model that allows for the earth's spherical geometry in full. Indeed, insofar as the Rossby waves on a β-plane are an accurate representation in midlatitudes of Rossby waves on a spherical earth, we can hope that our results have some quantitative validity as well.

When Rossby wave radiation occurs the shelf waves are damped. Although the damping rates incurred are not dramatic they are large enough to conclude that they may be significant for low-frequency shelf waves, particularly at high latitudes. This is consistent with the analysis by Enfield and Allen (1980) of sea-level anomalies along the Pacific Coast of America and with the numerical results of Suginohara (1981) and Suginohara and Kitamura (1984). How the damping rates due to Rossby wave radiation calculated here would compare with the damping rates due to local frictional effects is not known. For high-frequency shelf waves (i.e., periods in the range 2–10 days) Allen and Smith (1981) have estimated a frictional decay time of about 12 days for shelf waves off the Peru coast and about 7 days for shelf waves off the Oregon coast. For low-frequency shelf waves (i.e., periods in excess of 10 days) it seems likely that the frictional decay time will be larger, but comparable with the decay time due to Rossby wave radiation. Of the analytical approximations made in the model discussed in this paper, it is clear that the nondivergent approximation is the least serious; the inclusion of divergent terms would not significantly alter any of the conclusions in this paper. However, the restriction to barotropic waves is a severe limitation. Nevertheless, it seems clear that although the inclusion of stratification would make the analysis more complicated, the same general conclusions would apply. In particular, sufficiently low-frequency baroclinic shelf waves will lose energy due to radiating Rossby waves and the rate of energy loss will be determined by the radiated Rossby wave energy flux.

REFERENCES

Allen, J. S., 1980: Models of wind-driven currents on the continental shelf. *Annu. Rev. Fluid Mech.*, **12,** 389–433.

——, and R. L. Smith, 1981: On the dynamics of wind-driven shelf currents. *Phil. Trans. Roy. Soc. London,* **A302,** 617–634.

Beer, T., 1978: Non-divergent shelf-waves on the Ghana continental shelf. *Geophys. Astrophys. Fluid Dyn.*, **9,** 219–222.

——, and R. Grimshaw, 1983: Equatorward-propagating continental shelf waves. *J. Phys. Oceanogr.*, **13,** 1739–1743.

Buchwald, V. T., and J. K. Adams, 1968: The propagation of continental shelf waves. *Proc. Roy. Soc. London,* **305A,** 235–250.

Enfield, D. B., and J. S. Allen, 1980: On the structure and dynamics of monthly mean sea level anomalies along the Pacific Coast of North and South America. *J. Phys. Oceanogr.*, **10,** 557–577.

Grimshaw, R., 1977: The effects of a variable Coriolis parameter, coastline curvature and variable bottom topography on continental shelf waves. *J. Phys. Oceanogr.*, **7,** 547–554.

Holyer, J. Y., and L. A. Mysak, 1985: Trench wave generation by incident baroclinic waves. *J. Phys. Oceanogr.*, **15,** 593–603.

Ludwig, D., 1966: Uniform asymptotic expansions at a caustic. *Comm. Pure Appl. Math.*, **19,** 215–250.

McCreary, J. P., and S-Y. Chao, 1985: Three-dimensional shelf circulation along an eastern ocean boundary. *J. Mar. Res.*, **43,** 13–36.

Mysak, L. A., 1978a: Long-period equatorial topographic waves. *J. Phys. Oceanogr.*, **8,** 302–314.

——, 1978b: Equatorial shelf waves on an exponential shelf profile. *J. Phys. Oceanogr.*, **8,** 458–467.

——, 1980a: Topographically trapped waves. *Annu. Rev. Fluid Mech.*, **12,** 45–76.

——, 1980b: Recent advances in shelf wave dynamics. *Rev. Geophys. Space Science,* **18,** 211–241.

——, 1983: Generation of annual Rossby waves in the North Pacific. *J. Phys. Oceanogr.*, **13,** 1908–1923.

Pedlosky, J., 1979: *Geophysical Fluid Dynamics.* Springer-Verlag, 624 pp.

Suginohara, N., 1981: Propagation of coastal-trapped waves at low latitudes in a stratified ocean with continental shelf slope. *J. Phys. Oceanogr.*, **11,** 1113–1122.

——, and Y. Kitamura, 1984: Long-term coastal upwelling over a continental shelf-slope. *J. Phys. Oceanogr.*, **14,** 1095–1104.

Willmott, A. J., and A. A. Bird, 1983: Freely propagating trench waves on a beta-plane. *J. Phys. Oceanogr.*, **13,** 1659–1668.